AD-A152 820 EISCAT ELECTRON DENSITY STUDIES(U) LANCASTER UNIV 1/1
BAILRIGG (ENGLAND) DEPT OF ENVIRONMENTAL SCIENCES
J K HARGREAVES ET AL. 29 JAN 85 AFGL-TR-85-0052

UNCLASSIFIED F/G 4/1 NL

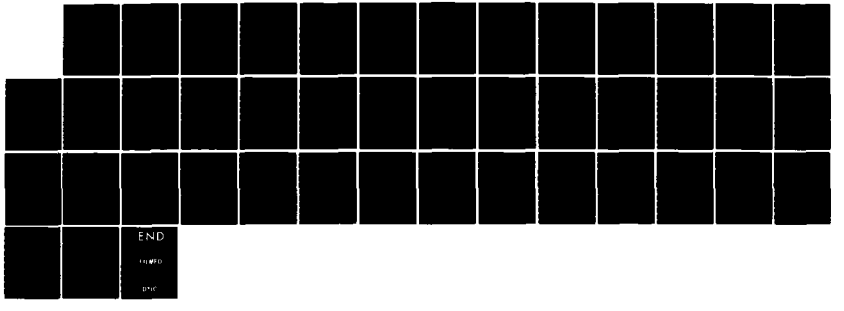

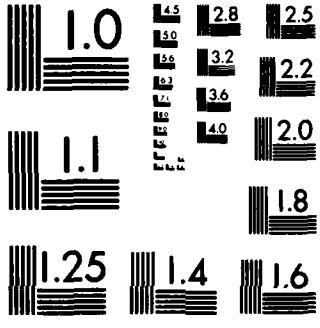

Grant AFOSR 83-0371

EISCAT ELECTRON DENSITY STUDIES

(Third Year)

J.K. Hargreaves and C.J. Burns,
Environmental Sciences Dept.,
University of Lancaster,
Lancaster LA1 4YQ
England.

29 January 1985

Final Report, 15 October 1983 - 29 January 1985.

Prepared for AFGL/PHY, Hanscomb AFB, MA 01731, U.S.A. and European Office of Aerospace Research and Development, London, England.

Contents

UNCLASSIFIED

SECURITY CLASSIFICATION OF THIS PAGE

REPORT DOCUMENTATION PAGE

1a. REPORT SECURITY CLASSIFICATION Unclassified	1b. RESTRICTIVE MARKINGS None
2a. SECURITY CLASSIFICATION AUTHORITY None	3. DISTRIBUTION/AVAILABILITY OF REPORT Approved for public release; distribution unlimited.
2b. DECLASSIFICATION/DOWNGRADING SCHEDULE None	
4. PERFORMING ORGANIZATION REPORT NUMBER(S) Environmental Sciences Dept., University of Lancaster, LancasterLA1 4YQ England	5. MONITORING ORGANIZATION REPORT NUMBER(S) AFGL-TR-85-0052
6a. NAME OF PERFORMING ORGANIZATION Air Force Geophysics Lab 6b. OFFICE SYMBOL (If applicable) LIS	7a. NAME OF MONITORING ORGANIZATION EOARD/LNG, Box 14, FPO New York 09510
6c. ADDRESS (City, State and ZIP Code) Hanscom AFB MA 01731	7b. ADDRESS (City, State and ZIP Code)
8a. NAME OF FUNDING/SPONSORING ORGANIZATION Air Force Geophysics Lab 8b. OFFICE SYMBOL (If applicable) LIS	9. PROCUREMENT INSTRUMENT IDENTIFICATION NUMBER AFOSR 83-0371
8c. ADDRESS (City, State and ZIP Code) Hanscom AFB MA 01731	10. SOURCE OF FUNDING NOS. PROGRAM ELEMENT NO.: 61102 · PROJECT NO.: 2310 · TASK NO.: G6 · WORK UNIT NO.: CC
11. TITLE (Include Security Classification) EISCAT Electron Density Studies	
12. PERSONAL AUTHOR(S) J.K. Hargreaves and C.J. Burns	
13a. TYPE OF REPORT Scientific. Final 13b. TIME COVERED FROM 150ct83 TO 29Jan85	14. DATE OF REPORT (Yr., Mo., Day) 29 Jan 85 15. PAGE COUNT 41
16. SUPPLEMENTARY NOTATION	

17. COSATI CODES		
FIELD	GROUP	SUB. GR.

18. SUBJECT TERMS (Continue on reverse if necessary and identify by block number)

Incoherent scatter radar; auroral zone; ionospheric F-region; small-scale plasma irregularities.

19. ABSTRACT (Continue on reverse if necessary and identify by block number)

Studies of the auroral ionosphere by incoherent-scatter radar have continued, with further observations of the fine structure of the F-region and with detailed analyses of data so obtained during the last three years. It has been demonstrated that irregular structures with scale sizes measured in kilometers can on occasion be detected by the EISCAT UHF radar to altitudes of at least 750 km, and first results on the magnitude, time structure, and velocity of these structures are presented. -> cont keywords to include:

20. DISTRIBUTION/AVAILABILITY OF ABSTRACT UNCLASSIFIED/UNLIMITED ☒ SAME AS RPT. ☐ DTIC USERS ☐	21. ABSTRACT SECURITY CLASSIFICATION Unclassified
22a. NAME OF RESPONSIBLE INDIVIDUAL John A. Klobuchar	22b. TELEPHONE NUMBER (Include Area Code) 617-861-3988 22c. OFFICE SYMBOL AFGL/LIS

DD FORM 1473, 83 APR EDITION OF 1 JAN 73 IS OBSOLETE.

UNCLASSIFIED

SECURITY CLASSIFICATION OF THIS PAGE

1. Introduction

The European Incoherent Scatter Radar (EISCAT) commenced operation in August 1981, and since that time several runs have been made of a Special Program (SP103) which is intended to observe the irregular structure of the high-latitude ionospheric F-region down to scale sizes of a few kilometers. The development of the Special Program began in May 1981 with support from the European Office of Aerospace Research and Development, and the present report is the third one describing progress. Following the development of the beam scanning program and analysis software, and the achievement of several runs, the recent period has seen five further runs, three of which coincided with overpasses of the HILAT satellite. Much effort has been expended during the reporting period in analysing and studying the data obtained in November 1982; more recent data have been partially processed.

This report summarises progress before October 1983 and then describes the work carried through during the third period of EOARD funding, October 1983-January 1985. The first scientific results and ideas for future work are summarised in Section 6. Details of the scientific analysis are contained in a paper (to be published in Radio Science) which is here included as Appendix 1.

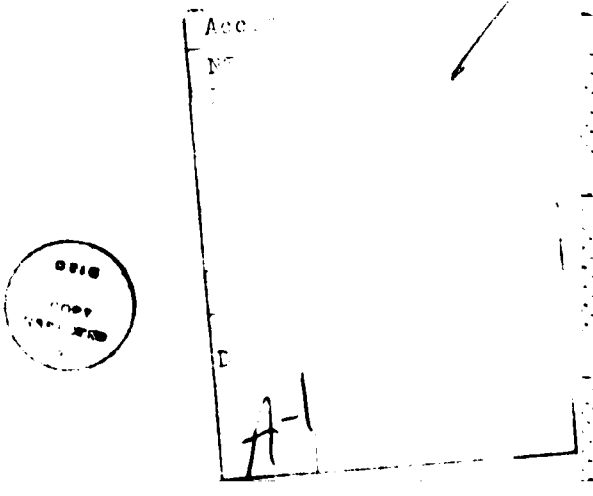

2. The project to October 1983

Work during the first year (May 1981 - 30 April 1982) and the second year (1 May 1982 - 30 April 1983) was supported by grants AFOSR-81-0049 and AFOSR-83-0054, and is described in previous reports (Hargreaves and Kirkwood, 1982; Kirkwood and Hargreaves, 1983). During the first year the feasibility of the observations was considered in some detail in terms of the likely magnitudes, scale sizes and drift speeds of irregularities, and the basic configuration of the EISCAT program was worked out. This was first run in December 1981, though the EISCAT system was still performing poorly at that time. The requirement to observe while the radar beam was being scanned presented the system with fresh problems to be solved, and the performance of the radar limited the scanning speed.

During the second year the data from December 1981 were studied in some detail, and several computer programs were developed. It was shown that the irregularities seen in these data were no larger than the noise expected from the radar parameters, and it was concluded that no ionospheric structures had been detected. The run had been made during magnetically quiet conditions. Another run was obtained in June 1981 during somewhat more active conditions but near noon. Again, no structure was seen. These early runs revealed a number of shortcomings in the EISCAT system, some of which were subsequently rectified. Two further (consecutive) runs in November 1982 were more successful in detecting irregularities, being made near midnight on a magnetically disturbed day. Some improvements were made to the EISCAT program, in particular by adding an E-region power profile. Attention was also given to the use of Common Program data for irregularity studies.

The Research Associate, Dr. S.C. Kirkwood, left Lancaster in May 1983 to take a position with the EISCAT Association at Tromsø. The project could not be continued until her successor, Mr. C.J. Burns, was appointed

in October 1983. Early 1983 was also a poor time for EISCAT observations, the entire facility being closed between January and September for major repairs. One consequence was that a run of SP103 that had been scheduled for January 1983 was not made until December. Long delays were also experienced in gaining access to EISCAT data tapes during these early years.

3. Special program for F-region irregularities

The concept of the experiment is to scan the radar beam rapidly in a north-south and east-west cross centred on the local geomagnetic field direction. The radar transmits and receives at Ramfjordmoen (69.6°N, 19.2° E), and there are receiving stations for tristatic operation at Kiruna (67.9°N, 20.4°E) and Sodankyla (67.4°N, 26.6°E). At 300 km range the arms of the cross extend 64 km. The beam is moved in 2 km steps, giving some beam overlap between successive points since the beamwidth of the UHF radar at 300 km altitude is 3 km. The beam spends 4 sec at each step, with 4 sec allowed for the antenna to move between steps, giving an effective scanning speed of 250 m/s at 300 km range. One full sweep takes 512 sec. The range resolution is 37.5 km.

The experiment is illustrated in Fig. 1 of Appendix 1, and the scanning sequence normally used is described in Section 1 of that Appendix.

4. Runs made, October 1983-January 1985

EISCAT work at the University of Lancaster is supported logistically by the EISCAT Group at the Rutherford Appleton Laboratory, and experiments are run during U.K. EISCAT campaigns. The experiment must first be approved and radar time allocated by the U.K. Time Allocation Panel. Seven runs were implemented between October 1983 and January 1985. Details are included in Table 1 which shows all the runs made so far.

Table 1 Summary of EISCAT runs of SP 103

Date	Time(UT)	Kp	Program	Comments
1981 Dec 17	1500 - 1700	2-	±50 km scans	System performing poorly. No irregularities seen. Analysed in detail and shown that variations no larger than system noise.
1982 June 3	1100 - 1300	2+, 2	±50 km scans	Daytime. No irregularities seen. No analysis planned.
1982 Nov 29-30	2115 - 0035 (2 runs)	5-, 4	±64 km scans	Irregularities present. Analysed for magnitudes, spectra and velocities.
1983 Dec 5-6	2310 - 0050	4-, 3+	±64 km scans E region	HILAT pass at 2333 UT. Data analysis in progress.
1984 Feb 9	2100 - 2300	3-	Searching mode	Tapes at RAL, not yet accessed. Electron densities low.
1984 Feb 10	2100 - 2300	5	±64 km scans E region	Data analysis in progress.
1984 Dec 15	0820 - 1100 (2 runs)	3/4*	"	Tapes at RAL, not yet accessed. HILAT pass at 0927 UT.
1984 Dec 15-16	2300 - 0150 (2 runs)	5/4*	"	Tapes at RAL, not yet accessed. HILAT pass at 0026 UT.

* Preliminary values

5. Analysis of special program data

Special program data can be analysed in two ways - either with the EISCAT analysis program where post-integration to 2 or more minuties is required, or with locally developed software where the original 4-second resolution is retained. The EISCAT analysis program is used to determine the ionospheric parameters electron density (Ne), electron temperature (Te), ion temperature (Ti) and composition, and ion drift velocity (Vi). The 4-second data consists of pseudo-electron densities.

Most of the work has involved the determination of the high-resolution data since this is of primary interest and is also indicative of the overall quality of data. Several stages of processing are required to obtain the data from a full run of an experiment. A brief summary of these stages is below.

5.1 Stages of data processing

(1) Finding the EISCAT tape

Raw data from a special program run are held on tape at the Rutherford and Appleton Laboratory at Didcot (RAL). The tape number is found by interrogating the EISCAT TAPES CATALOGUE which is available in the form of a menu-driven database on the NORD560 computer. The catalogue provides enough information to enable users to access the correct experiment files on the required tape. The tape resides either on the NORD560 or IBM computers and so a request to move it may be needed.

(2) Reading the EISCAT tape

The first step in reading an EISCAT tape for a particular run is to read the experiment description and news files. These are essential for determining how the raw data is stored on the tape and for keeping up to date with any changes made to the system. Some of the data processing programs contain experiment dependant parameters that may need to be changed from one run to the next. The experiment description files provide these.

Once these tiles have been read and checked the raw data can then be read from the tape. For a typical run of SP103 of 96 minutes duration the amount of data stored on tape is enormous. One data dump of 4 seconds alone contains 4223 32-bit words. Thus 96 minutes of data comprise 6,081,120 32-bit words. The result memory for 1 data dump is shown in Fig. 1. The data are usually organised into files of approximately 8 minutes in size, giving 12 raw data files on the tape. Not all of this data is needed to determine the pseudo-electron densities, only the zero-lags.

Each of the 12 data files is read and stored on a temporary disk where files remain for a maximum of 28 days. During this time the files can be accessed and the zero-lags read and stored in the user's personal directory. This file is only about 1/25 the length of the original file, but still amounts to some 1400 lines of printout for 8 minutes of data.

(3) Checking the data

The program that reads the zero-lags from the temporary disk also checks signal attenuation and filter settings and prints out warnings if these are not correct. Since 3 single pulse frequences are used in the experiment the program will read all 3 sets of zero-lags. The background and calibration details are also read. If power profile data are required the program can be easily changed to read these instead.

(4) Cleaning the data

The 3 single pulse frequences have been used in the experiment to increase the signal/noise ratio. These 3 sets of zero-lag range gates, calibration gates and background gates are combined into one set. The calibration and background gates are then averaged and the background gates smoothed. Excessively low or high transmitter power values (> 20% from normal) are removed and any large spikes in the zero-lags are also removed. These will most likely be caused by satellite echoes

Figure 1

THE STRUCTURE OF A 4-SECOND DATA DUMP FOR SP103

USING CORRELATOR PROGRAM PROG13

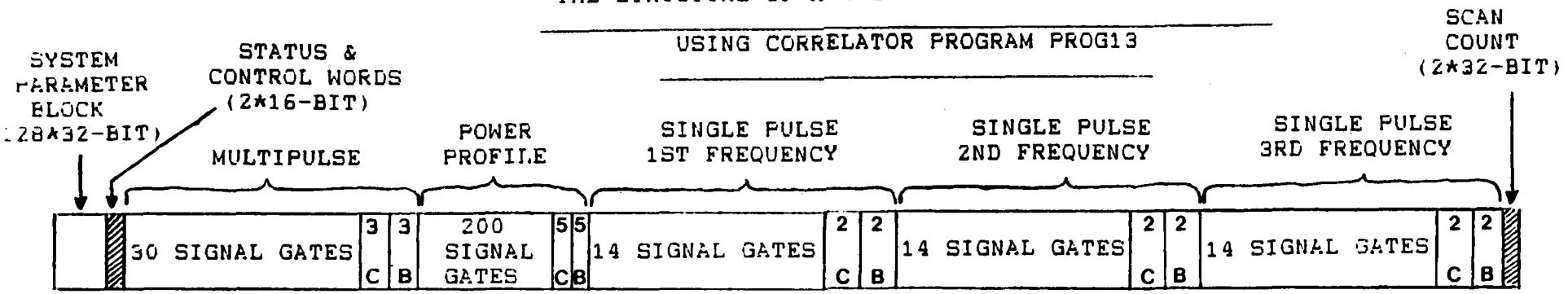

C=CALIBRATION GATE

B=BACKGROUND GATE

MULTIPULSE GATE

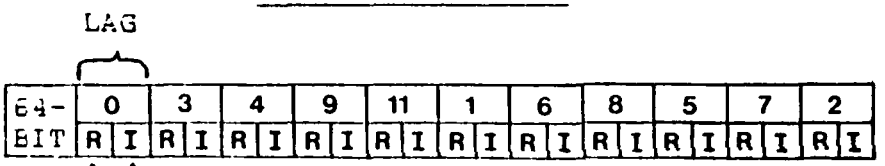

POWER PROFILE GATE

R=REAL

I=IMAGINARY

SINGLE PULSE GATE

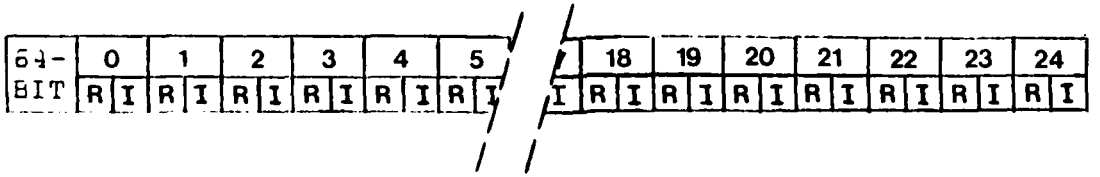

TOTAL NO. OF 32-BIT WORDS = 4223

or instrumental faults. The resultant data file will thus contain cleaned data ready for converting into electron densities.

(5) Converting the data to electron densities

The final stage in the processing of data is quite simple. The cleaned raw data are converted into electron densities by range correction. The formula used is given in section 5.2.

Each 8-minute data file is processed individually in this way, and the final data file is gradually built up until it contains the full 96 minutes of data.

5.2 Programming

At the start of the year several amendments to existing programs were required due to changes in the EISCAT system of recording information on tape. A new version (no. 4) of the system parameter-block was implemented in January 1983 which meant that the tape for the December 1983 run of SP103 would have to be read with the amended programs. In addition to these amendments a new method of calculating electron densities has been employed due to the increased reliability of the calibration injection (from July 1983). Until this time a scaling factor found from an ionosonde was used to scale the electron densities. Assuming that Te/Ti=1 then:

$$Ne = \frac{(S-B)}{(C-B)} * \frac{Tcal*KB*RXBW*2*R^2*SYSC}{PL*PPWR}$$

Where S = zero lag of signal
B = zero lag of background (average)
C = zero lag of calibration (average)
Tcal = calibration temperature (205 K)
KB = Boltzman's constant (1.38 E-23)
RXBW = receiver bandwidth (0.25 E+05 Hz)
R = range in metres
SYSC = system constant (1.38 E+19)
PL = length of transmitted pulse (0.25 E-03 s)
PPWR = peak transmitter power in watts.

Programs written during the reporting period are briefly described in Appendix 2, which also tabulates the main programs now available.

5.3 Hardware Developments

The main facilities now available for data analysis are:-

MAINFRAME COMPUTERS

Rutherford & Appleton Laboratory (RAL)	(1) IBM 3032 (2) NORSK DATA 560
University of Lancaster	(1) VAX 11/780 (2) ICL 2960

MICRO COMPUTERS

University of Lancaster	DIGITAL PROFESSIONAL 350

GRAPHICS OUTPUT

University of Lancaster	(1) DIGITAL VT101 TERMINAL (2) ASCOT TERMINAL (3) MELLORDATA MICROCOLOUR (4) TEKTRONIX 4662 COLOUR PLOTTER (5) CALCOMP PLOTTER

In late 1983 a GEC 4160 computer was installed on campus at Lancaster to operate as a Campus Packet Switch Exchange. Most of the mainframe computers on campus are connected to this switch. The campus network is also connected into mainframes outside the University (e.g. the Amdahl in Manchester) and to external networks (e.g. the Joint Academic Network, known as JANET). A number of devices called PADs (Packet Assembler/ Disassemblers) have been installed around the campus to allow up to 16 terminals to be joined to one single cable leading to the central switch. So far 5 PADs have been installed and are operational, allowing any of 80 Lancaster terminals to connect to just about every computer in UK universities and the Research Councils.

Networking software has been commissioned on most mainframe computers on the network to provide file transfer between computers such as the IBM at RAL and the VAX at Lancaster. In the past year it has been possible to process data on the IBM and then transfer it to the VAX for analysis

thus making use of the facilities listed above. One advantage of using these facilities as opposed to those at RAL is the much faster turn-around time for hardcopy output.

For use with this project a Digital Professional 350 micro-computer has been set up to emulate a VT101 terminal allowing the micro to communicate with any mainframe computer on the network. This has enabled data and/or programs to be stored on the micro's own disks for a permanent record or for use with software developed on the micro.

These developments represent an enormous step forward for the computer user at Lancaster, and they greatly strengthen the ability of even small research groups to undertake research projects involving major data analysis. The present project is already reaping considerable benefits from the computer developments of the last year.

5.4 Present state of data processing

The runs of November 1982 continued to be studied as the first priority, since the first look has indicated the presence of strong irregularities (Kirkwood and Hargreaves, 1983, Fig. 5). The electron density values were organised to indicate the magnitude of irregularities in relation to the mean electron density, as a function of height. Auto-correlation functions and power spectra were determined, again as functions of altitude. Examples are shown in Appendix 1, Figs. 3 and 4.

Drift velocities had already been estimated from the tristatic Doppler data; though, on the basis of the scatter between determinations using the three sounding frequences independently (Kirkwood and Hargreaves, 1983), it was felt necessary to assign rather large error bars to these velocities - See Table 3 of Appendix 1. An independent method of velocity determination makes use of the magnetic field alignment of the irregularities, which implies that the range of a selected irregularity should change with time as it drifts through the radar beam, the beam

being inclined to the magnetic field direction. The method is illustrated and some results are shown in Appendix 1, Figs. 5 and 6.

The data from later runs have been processed in a similar manner as far as time has allowed. Table 2 summarizes the current state of reduction of each run made since 1981.

5.5 Future data processing

From the spectral analysis carried out so far very few if any periodicities are seen below about 15 seconds. It is therefore planned to filter the data to remove anything below 15 seconds and as a result obtain cleaner data. Alternative data presentations are being considered.

The RAL EISCAT analysis program will be used for determining drift velocities and electron/ion temperatures. The new RAL NORD computer recently installed (mid 1984) should enable more efficient data processing since it has been set up for specific use by the EISCAT community in the U.K.

Now that we have received a HILAT summary tape we should be in a position to analyse data from the HILAT pass of December 1983, comparing it with the data obtained from our experiment run simultaneously. Four further runs of our experiment have been made very recently (December 1984) with simultaneous overpasses of HILAT, and these promise to be of even better quality. Precipitation events occurred during these runs, so it may be possible to assess the contribution of local precipitation to the F-region irregularities.

Table 2

Present State of Processing and Analysis of Data

DATE OF START OF EXPERIMENT	READ FROM TAPE	DETERMINED ELECTRON DENSITIES	DETERMINED POWER SPECTRA	DETERMINED Vi,Ti, Te etc.	HILAT DATA
1981 DEC 17	YES	YES	NO	NO	-
1982 JUN 3	YES	YES	NO	NO	-
1982 NOV 29 (2 runs)	YES	YES	YES	YES	-
1983 DEC 5	YES	YES	YES	NO	RECEIVED
1984 FEB 9	NO	-	-	-	-
1984 FEB 10	YES	YES	NO	NO	-
1984 DEC 15 (2 runs)	NO	-	-	-	REQUESTED
1984 DEC 16 (2 runs)	NO	-	-	-	REQUESTED

6. Reports and Publications: First scientific results

6.1 Reports

The following reports have been given on the experiments and results.

C.J. Burns, J.K. Hargreaves and S.C. Kirkwood: High-latitude F-region irregularities observed by EISCAT in November 1982. Talk at meeting on Magnetosphere, Ionosphere, and Solar-Terrestrial Physics, Leicester (April 1984).

J.K. Hargreaves, C.J. Burns and S.C. Kirkwood: EISCAT studies of F-region irregularities using beam scanning. Workshop on Irregularities in the High-Latitude Ionosphere, Katlenburg-Lindau (September 1984). Written version accepted for special issue of Radio Science. (Copy attached as Appendix 1).

6.2 First results

The first results from the Special Program runs are described in Appendix 1, and may be summarised as follows:-

(1) The irregularities are observed more strongly at times of geomagnetic disturbance. None have yet been detected if $Kp < 3$. This applies only to night-time runs and little can be said at present about the daytime behaviour.

(2) The irregularity intensity varies greatly from time to time, even within tens of minutes. The standard deviation of electron density at given height may amount to 30-40% of the mean electron density; at other times it may be no more than a few percent and not measurable above the experiment noise.

(3) The irregularities are more intense at the greater altitudes. As a percentage of the mean electron density the irregularity intensity appears to increase with height indefinitely. In absolute terms there may be a maximum somewhat above the F-region peak. Despite increasing measurement noise, irregularities may be detected up to (at least) 750km

(4) Plots showing the variation of electron density with time at given altitude often give the visual impression of wavelike variations, and power spectral analysis tends to support this. In the data analysed so far, a periodicity near 1 minute appears more often than would be expected. A spatial wavelength of 15 km is implied if the drift speed is 250 m/s.

(5) Velocity components in the plane of the scan can be determined, since the irregularities are field-aligned. The first results from this analysis are not inconsistent with the velocities determined from tristatic Doppler shifts in most cases, though some sections are difficult to interpret and may indicate that the drift contains an oscillating component.

6.3 Further analysis and experiments

From the experience gained so far it is recommended that future work should be along the following lines.

(1) Continue to analyse data from the runs already made, concentrating on irregularity magnitudes, periodicities, and velocities; also ion and electron temperatures and plasma drift.

(2) Compare these results with data from the coincident HILAT passes. Make further runs during HILAT passes.

(3) Incorporate E-region data in the analysis.

(4) Devise and implement new observing programs, possibly involving the forthcoming VHF radar in addition to the UHF radar, to learn more about the irregularity shapes and sizes.

(5) Observe in conjunction with other space vehicles such as GPS and SIR-B.

(6) Survey irregularity occurrence from the body of Common Program data: CP1, which operates with the beam stationary along the local field line; CP3, which makes a wide north-south scan covering 10° of latitude.

References

J.K. Hargreaves and S.C. Kirkwood: EISCAT Electron Density Studies - final report for 1 May 1981-30 April 1982.
University of Lancaster report (June 1982).

S.C. Kirkwood and J.K. Hargreaves: EISCAT Electron Density Studies (Second Year) - final report for 1 May 1982-30 April 1983.
University of Lancaster report (May 1983).

(Further references are included in Appendix 1, pages 12-13).

To be published in Radio Science (1985)

Appendix 1

EISCAT studies of F-region irregularities using beam scanning

J.K. Hargreaves, C.J. Burns and S.C. Kirkwood*

Environmental Sciences Dept.,
University of Lancaster,
Bailrigg, Lancaster. LA1 4YQ, England.

Abstract

A beam scanning program to study the F-region irregularities of smaller scale has been run on the EISCAT UHF radar. At the 300 km level the scan covers 128 km in about 8½ minutes, there being north-south and east-west scans as well as periods with the beam stationary and directed along the local magnetic field direction.

The paper gives examples of the variations of electron density observed at given ranges during a geomagnetically disturbed period. Power spectra suggest the presence of periodicities from one to several minutes during some sections of the runs. It is demonstrated that the velocities of field-aligned irregularities can be determined from their observed range-time behaviour, and measurements made thus are compared with the plasma drift determined from tristatic reception. The irregularity motions appear to vary considerably during the time of one 8½-minute scan, and in some cases may indicate a propagating wave.

* Now at EISCAT Scientific Association, Tromsø, Norway.

1. Introduction

One of the distinguishing features of the high-latitude ionosphere is a high degree of spatial irregularity over many distance scales and with varying intensity. Much of the information about F-region irregularities has come from ground-based studies of radio wave scintillation (Aarons, 1973) and from in-situ measurements by satellites and rockets (Clark and Raitt, 1976; Phelps and Sagalyn, 1976). Such measurements have provided information on the geographic, time-of-day, seasonal and magnetic activity dependence of irregularity occurrence, on their size distributions, and some studies have been made of their shape and alignment (Fremouw and Lansinger, 1981; Rino and Vickrey, 1982; Livingston et al., 1982).

An incoherent scatter radar can measure electron density for extended periods of time, over a range of heights simultaneously, and over a range of geographic locations, and thus provides a means to observe heights, sizes, shapes, alignments, drifts and lifetimes, as well as adding statistical information on occurrence and intensity. Properties such as temperature and field-aligned ion motion can also be determined, information which is invaluable in relation to theories of irregularity formation (Frihagen, 1969, 1971; Kelley and Kintner, 1978; Reid, 1968; D'Angelo and Motley, 1961; Hudson and Kelley, 1976). Kelley et al. (1982) have defined three size ranges of F-region irregularities: "large scale", >10 km; "medium scale", 100 m - 10 km; and "small scale", <100 m. Because of its beamwidth, incoherent scatter radar can only observe the structures of large and medium scale, and work at Chatanika has principally concerned the larger structures, sometimes called "blobs" (Kelley et al., 1982; Muldrew and Vickrey, 1982; Tsunoda and Vickrey, 1983).

To explore the F-region irregularities in the high-latitude ionosphere a program has been developed for the EISCAT UHF (933 MHz) incoherent-scatter radar which scans the beam north-south and east-west in a cross centered on the local magnetic field direction. The radar transmits and receives at Ramfjordmoen (69.6°N, 19.2°E) near Tromsø, Norway, and there are receiving stations for tristatic operations at Kiruna, Sweden (67.9°N, 20.4°E) and Sodankylä, Finland (67.4°N, 26.6°E). As illustrated in Figure 1, the arms of the cross extend 64 km at the 300 km level, and the beam is moved along in 2 km steps. With 4 sec. on each step and another 4 sec. allowed for the antenna to move between steps - though data are taken all the time - the beam velocity is effectively 250 m/s at 300 km range, and one full sweep, for example from south to north, takes 512 sec. (8.53 min). The range resolution is 37.5 km and data are taken over ranges between 184 and 746.5 km.

Since the local magnetic field is inclined 13.5° to the vertical, the elevation scan (Fig. 1a) takes the beam from 64° elevation to nearly vertical. It is not practical to drive the UHF dish directly through the zenith in a rapid scan experiment. Figure 1(b) shows the azimuth (east-west) scan as planned. One complete run was made up of a sequence of scans that included some periods when the beam was stationary (St) and directed along the local magnetic field direction, as follows:

St, S→N, N→S, S→N, N→S, St, E→W, W→E, E→W, W→E, St.

Each of these we call a "section" of the run. The whole run, comprising 11 sections, takes a little over 1½ hrs. In some of the runs to be discussed the azimuth scan was only one quarter of that intended and those data approximate more to the case of a stationary beam.

2. Observations effected

Between December 1981 and February 1984 the experiment was run on 6 occasions, as in Table 1.

Table 1: Runs of beam-scanning F-region program

Date	Time (U.T.)	Kp	Comments
1981 Dec 17	1500 - 1700	2-	Scans of ± 50 km
1982 June 3	1100 - 1300	2+,2	Scans of ± 50 km
1982 Nov 29-30	2115 - 0035	5-,4	Scans of ± 64 km N-S and ± 16 km E-W. Two runs made.
1983 Dec 5-6	2310 - 0050	4-,3+	Scans of ± 64 km. Also E-region data. HILAT pass.
1984 Feb 9	2100 - 2300	3-	Searching mode.
1984 Feb 10	2100 - 2300	5	Scans of ± 64 km. Also E-region data.

On some occasions no measurable irregularities were present. A detailed analysis of the run of 1981 Dec 17 led to the conclusion that the fluctuations recorded were no larger than the experimental noise level governed by the parameters of the radar. This was early in the operation of the EISCAT system, which had first been used the previous August and was not yet operating up to specification. The run of 1982 June 3 was near the middle of the day in summer when the F-region was controlled by solar radiation; no irregularities were observed during this run. Both of these runs were during magnetically quiet periods.

3. Results from 1982 November 29-30

3.1 Average electron density profiles

On 1982 November 29-30 the experiment was run twice. Figure 2 shows the average electron density* profiles for the six 8½-minute sections when the beam was stationary. There was some variation with time in the average profile, most of which occurred near the beginning of

* Strictly these are the "raw" electron density values, not corrected for the ion

Run I. During Run II the variation was only about 40%. These profiles are not exceptional in any regard; nor is there any obvious relation between the profile shape and the presence or absence of irregularities. Referring to the profiles in Figure 2, irregularities were relatively weak during the third period of Run I and during the second period of Run II; during the other periods the irregularities were relatively large.

3.2 Magnitude of irregularities

Figure 3 presents examples of the observations with the beam stationary. In this format each plot of electron density at given height is adjusted so that the mean electron density over that section is plotted opposite the relevant height mark. In the first example structure is obviously present, the standard deviation amounting to as much as 30% to 40% of the mean. There appears to be some regularity in the structure. The second example is much smoother; the standard deviation here is no more than 10-20% of the mean, only a few percent at the lowest levels.

With increasing height there is an increasing contribution of noise. This may be taken approximately into account by assuming that during the quietest periods all the variance is due to noise. Subtracting those values, height for height, from the variance during the more disturbed periods then leads to estimates of the variance and standard deviation due to ionospheric irregularities. Applied to the measurements of November 29-30, this procedure leads to the conclusion that the standard deviation is not constant with respect to height, but that the ratio (standard deviation)/mean increases steadily with height from less than 10% at the lowest altitude (184 km) to 20-30% at the highest (746.5 km). In absolute terms the irregularities tend to be largest between 350 and 550 km, altitudes above the maximum of the mean electron density. The foregoing results are for filtered data from which periodicities longer than about 2 minutes have been removed.

From the limited data so far available it appears that the presence and intensity of F-region irregularities is related to the general level of geophysical disturbance. During the runs of 1982 Nov. 29-30 there was locally a geomagnetic disturbance which had been more intense several hours before the first run began but which nevertheless continued during both runs. The H-component of the Tromsø magnetometer (Auroral Observatory, Tromsø, 1982) was more disturbed during Run I than during Run II. The riometer of the University of Lancaster operating at Abisko, Sweden, 120 km south of Ramfjord, showed a small auroral absorption event reaching 0.68 dB during Run I (2115-2251 UT), and the decay of this event coincided with the reduction in the intensities of irregularities towards the end of that run. The irregularities were generally weaker throughout Run II (2300-0036UT)and during this period the riometer showed only slight activity, reaching 0.18 dB near the beginning of the run when the irregularities were in fact strongest. The correlation coefficient between the absorption measured by the riometer, and the standard deviation of electron density at a fixed height (409 km), is 0.44, which is statistically significant at the 5% level. Although the riometer and the magnetometer monitor the lower ionosphere rather than the F-region, these associations suggest that the F-region irregularities are associated with local activity, though that may, of course, be only part of a wider disturbance. Hargreaves and Hunsucker (1981) have previously reported an association between events on riometers and night-time enhancements of electron content determined from the ATS-6 radio beacon experiment.

3.3 Power spectra

To quantify the time variations seen in diagrams like Figure 3, power spectra have been formed for each range of each section of each run. Those in Figure 4(a) correspond to the data of Figure 3(a). The

spectra are seen to change only gradually with range, confirming (since the beam was pointed along the local geomagnetic field at this time) that the irregularities tend to be field aligned. These spectra show distinct periodicities of 152 sec. and 65 sec. The spectra in Figure 4(b), which are for a time of weak irregularities, do not show this coherence from one range to the next.

Table 2 summarises the periodicities that are most apparent in the 11 sections (see Introduction) of each run. Sections having significant breaks in the data were not included.

Table 2: Periodicities and ranges of strongest occurrence

Run I			Run II		
Section	Period(s)	Range(km)	Section	Period(s)	Range(km)
1	65	184-409	2	126	297-709
	152	372-597	4	205	184-672
2	58	447-559	5	56	447-634
3	115	372-709		251	334-597
8	53	297-559	7	237	259-709
	202	297-672	8	77	334-597
9	58	409-709		181	297-747
			9	55	484-597
				256	184-597
			10	251	184-634

Of 12 spectra showing significant peaks, 6 include a periodicity near 60 second (from 53 to 65). No other peak occurs so often, the next most frequent being three occurrences near 250 seconds. It is not clear what significance can be attached to these well defined periodicities, though their presence is interesting and because of them the spectra do not have the appearance that might have been expected. (See, for

example the spatial spectrum derived by Kelley et al. (1982)). It is also noted in Figure 4 that the spectral power attributed to irregularities is confined to frequencies less than 20 units, corresponding to periods greater than 25 seconds. This holds true for all sections of the data.

3.4 Velocities from tristatic data

Assuming that the observed electron density fluctuations are caused by spatial structure drifting through the beam, then a knowledge of the drift speed would give us the spatial wavelengths of the structures. The experiment was tristatic, with the remote stations at Kiruna and Sodankylä receiving the signals scattered from the 300 km level. From these tristatic data the plasma drift speeds were obtained during the sections of the runs when the beam was stationary. The resulting drift speeds, with error estimates, are given in Table 3.

Table 3: Velocities determined from tristatic observations

U.T.	Velocity (m/s)		
	Eastward	Southward	Total horizontal
2115 - 2123	278 ± 331	210 ± 122	348 ± 274
2159 - 2207	237 ± 104	278 ± 58	365 ± 81
2242 - 2250	105 ± 76	88 ± 60	137 ± 70
2300 - 2308	274 ± 72	-36 ± 208	276 ± 76
2344 - 2352	-94 ± 99	68 ± 70	116 ± 97
0028 - 0032	-34 ± 110	109 ± 104	114 ± 105

The error bars are relatively large, but there is enough consistency to suggest eastward drift to 2308 U.T. followed by a slower westward drift. The meridional component was essentially southward except for a possible northward excursion at 2300-2308 U.T. The total horizontal speed changed from approximately 350 to 115 m/s.

If 250 m/s is taken as a typical drift speed, a period of 60 sec corresponds to a spatial wavelength of 15 km, and 240 sec corresponds to 60 km. These irregularities therefore appear to be somewhat smaller than the "blobs" discussed by Kelley et al. (1982) among others, though they could of course be part of the structure within, or related to, "blobs".

It is observed from the power spectra that the experiment detects no significant irregularities at periods shorter than 25 sec. With a speed of 250 m/s this would correspond to a spatial wavelength of 6.25 km. Since the beamwidth of the UHF beam is only 3 km at range 300 km it seems unlikely that the beamwidth is limiting the present data.

3.5 Velocity determination from beam scanning

If the radar beam were scanned in elevation through stationary field-aligned irregularities, the structures would be seen to follow a range-time diagram like that shown in Figure 5(a). The details of the diagram would depend on the magnitude of the north-south velocity; two examples, $v = \pm 250$ m/s, are given as Figures 5(b) and (c). We have taken the convention that v is positive if the irregularities move in the same direction as the beam. In Figure 5(c) the horizontal line appears where the beam velocity matches the irregularity velocity. Another limiting case occurs if $v = \pm \infty$, when all the lines on the diagram become vertical.

Patterns similar to Figure 5(b) were seen in several of the south-to-north scans, Figure 6(a) for 2309-2317 UT being one example. In this case the lines drawn through what appear to be related peaks or troughs correspond (from left to right) to velocities of 63, 59, -307, -66, -213, -197, -161 m/s. Here, positive velocity means northward movement. There is an apparent change of direction from northward to

southward, which would be consistent with the change between 2300-2308 UT and 2344-2352 UT shown in Table 3. Considering the uncertainties too much stress should not at this stage be laid on detailed differences of value, but it does appear that changes can occur abruptly.

Scans from north to south do not always fit the pattern so well, Figure 6(b) being perhaps the most striking example. The six lines marked on this figure correspond to velocities of -180, -2143, 462, 944, 1900, -2753 m/s. Positive velocity here means southward movement. It must be remembered that if the beam is moving at nearly the same speed as the irregularities in the north-south plane the time variations could be due mainly to an east-west component of the velocity. It does not appear possible to account for the pattern of Figure 6(b) by means of a steady drift. One possibility is that the drift speeds were indeed large and rapidly changing but an alternative is that the pattern may be produced by a wave propagating in the east-west direction such that enhancements or depletions of electron density move alternately northward and southward with respect to the radar beam. Near 150 sec. and again near 380 sec. on figure 6(b) can be seen enhancements at lower altitudes at the same times as depletions at higher levels. These suggest that enhancements and depletions are adjacent to each other, and are observed simultaneously at different ranges because of the inclination of the beam to the geomagnetic field. Wave motions appear to be the best explanations of the features around 150, 280 and 380 seconds. Other sections of the Nov. 29-30 runs do not appear to require a special explanation, and 2132-2140 UT may, therefore, have been exceptional.

4. Conclusions

1. Irregularities in the F-region electron density have been observed at EISCAT under conditions of geomagnetic disturbance. There is evidence that the level of local activity is significant as well

as the planetary level. No irregularities have yet been detected for Kp < 3.

2. The irregularities become more intense, relative to the mean electron density, with increasing altitude. Although the measurements become noisy at the highest levels, irregularities may be detected up to (at least) 750 km. In absolute terms their intensity tends to be greatest somewhat above the F-region peak.
3. Power spectra support the visual impression that some irregularities have a wavelike character. A periodicity near 1 minute occurs rather frequently in the spectra. Taking 250 m/s as a typical drift speed this corresponds to a spatial wavelength of 15 km.
4. The irregularities being essentially field-aligned, it is possible to determine velocity components in the plane of the beam scan. First results are not inconsistent with the plasma velocity determined from tri-static data, but some sections are difficult to interpret and may indicate the passage of a wave.

Acknowledgements

These experiments were run at EISCAT during U.K. campaigns and thanks are due to the EISCAT Group at the Rutherford Appleton Laboratory for their support. The project has been funded by the Air Force Office of Scientific Research under grants 81-0049, 83-0054 and 83-0371.

References

Aarons, J.

A descriptive model of F layer high-latitude irregularities as shown by scintillation observations. J. Geophys. Res. 78, 7441 (1973).

Auroral Observatory, University of Tromsø, Norway.

Magnetic records, November 1982. Report ISSN 0332-6098.

Clark, D.H. and W.J. Raitt.

The global morphology of irregularities in the topside ionosphere as measured by the total ion current probe on Esro-4. Planet. Space Sci. 24, 873 (1976).

D'Angelo, N. and R.W. Motley.

Electrostatic oscillations near the ion cyclotron frequency. Phys. Fluids. 5, 633 (1962).

Fremouw, E.J. and J.M. Lansinger.

Dominant configurations of scintillation producing irregularities in the auroral zone. J. Geophys. Res. 86, 10087 (1981).

Frihagen, J.

Irregularities in the electron density of the polar ionosphere. The Polar Ionosphere and Magnetospheric Processes, G. Skovli (ed), p.271. Gordon and Breach (1970).

Hargreaves, J.K. and R.D. Hunsucker.

Night-time enhancements of ionospheric electron content at L=4 during substorms. Geophys. Res. Lett. 8, 815 (1981).

Hudson, M.K. and M.C. Kelley.

The temperature gradient drift instability at the equatorward edge of the ionospheric plasma trough. J. Geophys. Res. 81, 3913 (1976).

Kelley, M.C. and P.M. Kintner.

Evidence for two-dimensional inertial turbulence in a cosmic scale low β plasma. Astrophys. J., 220, 339 (1978).

Kelley, M.C., J.F. Vickrey, C.W. Carlson and R. Torbert.

On the origin and spatial extent of high-latitude F-region irregularities. J. Geophys. Res. 87, 4469 (1982).

Livingston, R.C., C.L. Rino, J. Owen and R.T. Tsunoda.

The anisotropy of high-latitude night-time F region irregularities. J. Geophys. Res. 87, 10519 (1982).

Muldrew, D.B. and J.F. Vickrey.

High-latitude F-region irregularities observed simultaneously with ISIS 1 and the Chatanika radar. J. Geophys. Res. 87, 8263 (1982).

Phelps, A.D.R. and R.C. Sagalyn.

Plasma density irregularities in the high-latitude topside ionosphere. J. Geophys. Res. 81, 515 (1976).

Reid, G.C.

The formation of small scale irregularities in the ionosphere. J. Geophys. Res. 73, 1627 (1968).

Rino, C.L. and J.F. Vickrey.

Recent results in auroral-zone scintillation studies. J. Atmos. Terr. Phys. 44, 1982.

Tsunoda, R.T. and J.F. Vickrey.

Evidence of east-west structure in large-scale F-region plasma enhancements in the auroral zone. Private Communication (1983).

CAPTIONS

1. Scans of the UHF radar beam. Each scan is composed of 64 steps and takes 512 seconds:

   (a) Elevation (N-S) scan; (b) Azimuth (E-W) scan.

2. Mean electron density profiles during periods when the beam was stationary along the field-line, for both runs on 1982 Nov. 29-30.

3. Examples of electron density variations seen with stationary beam: (a) 2115-2123 UT, showing strong irregularities; (b) 2242-2251, showing weak irregularities. In each case the mean electron density at given height is plotted at the relevant height mark and the variations about the mean are as shown on the scale. The mean electron density profiles over these periods are in Figure 2.

4. Normalised power spectra for the stationary-beam observations shown in Figure 3, mean and linear trend having been removed: (a) 2115-2123, showing periodicities at 152 sec and 65 sec; (b) 2242-2251, showing mainly noise. The unit of frequency is 1.98×10^{-3} Hz.

5. The models of the range-time patterns expected in elevation scans if the ionosphere contains field-aligned irregularities moving in the plane of the scan at velocity v. A given irregularity should be seen to move along, or parallel to, one of these curves. Velocity is positive for irregularities moving in the same direction as the beam, and negative for movement in the opposite direction.

   (a) $v = 0$; (b) $v = -250$ m/s; (c) $v = +250$ m/s.

6. Range-time patterns observed during azimuth scans.

   (a) South-to-north scan, 2309-2317 UT, showing evidence of moving field-aligned structures.

   (b) North-to-south scan, 2132-2140 UT, showing a more confused pattern.

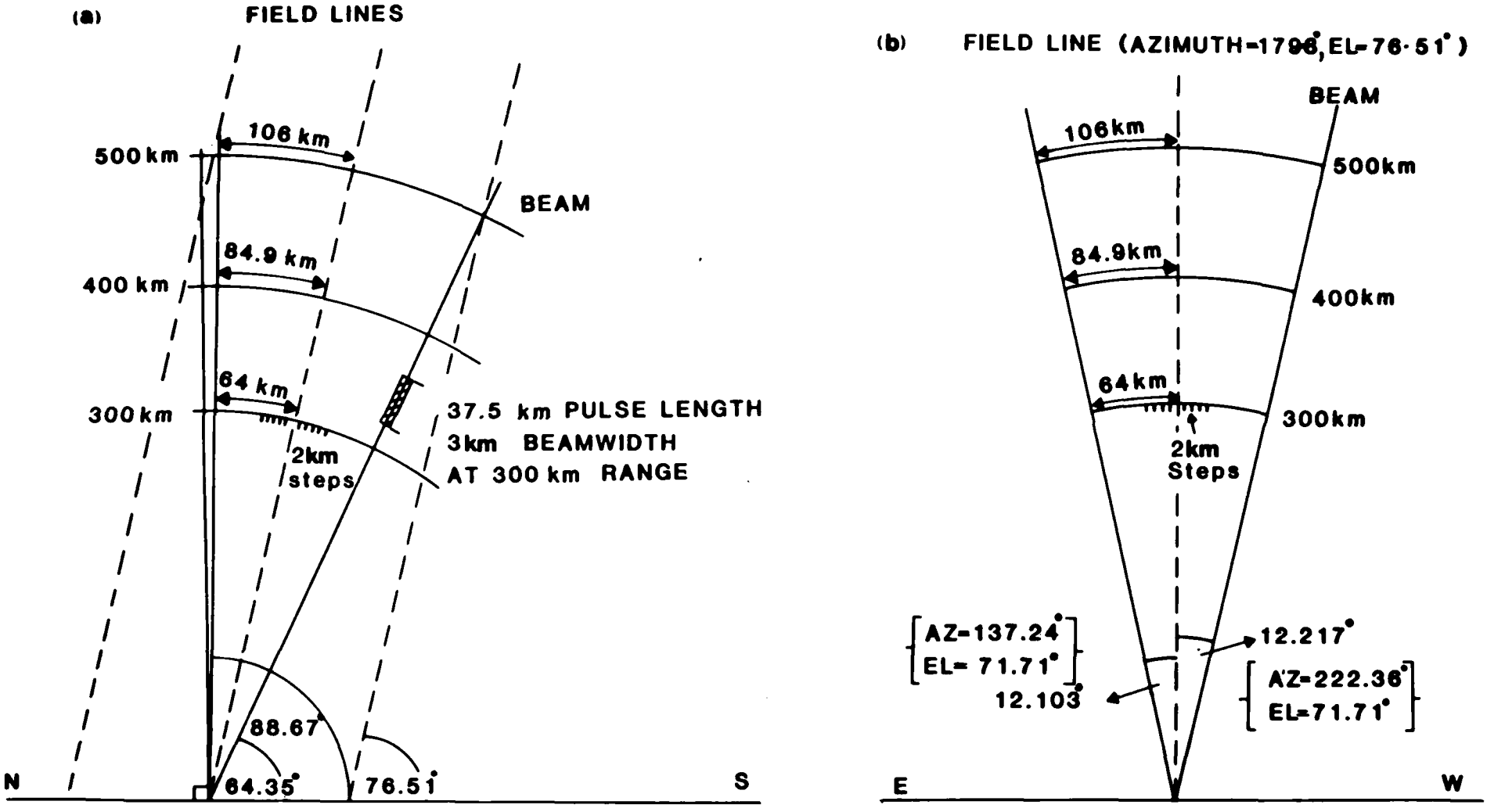
(a)
FIELD LINES
106 km
500 km
BEAM
84.9 km
400 km
64 km
300 km
37.5 km PULSE LENGTH
3km BEAMWIDTH
AT 300 km RANGE
2km
steps
88.67°
64.35°
76.51°
N
S
(b)
FIELD LINE (AZIMUTH=179.6°, EL=76.51°)
BEAM
106km
500km
84.9km
400km
64km
300km
2km
Steps
AZ=137.24°
EL= 71.71°
12.103°
12.217°
AZ=222.36°
EL=71.71°
E
W

Fig. 1

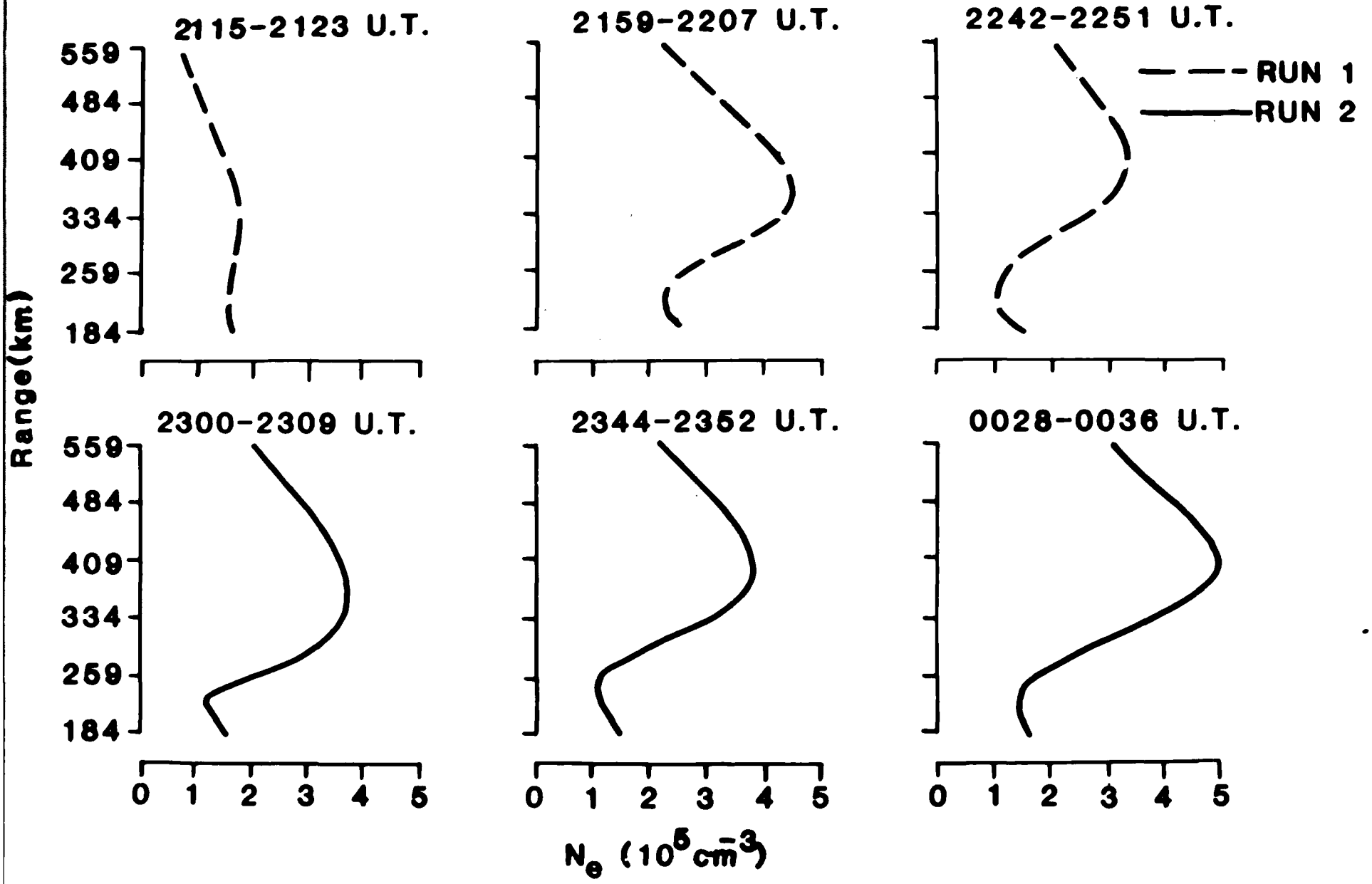
2115-2123 U.T.
2159-2207 U.T.
2242-2251 U.T.
RUN 1
RUN 2
2300-2309 U.T.
2344-2352 U.T.
0028-0036 U.T.
Range(km)
559
484
409
334
259
184
0 1 2 3 4 5
N_e ($10^5 cm^{-3}$)

Fig. 2

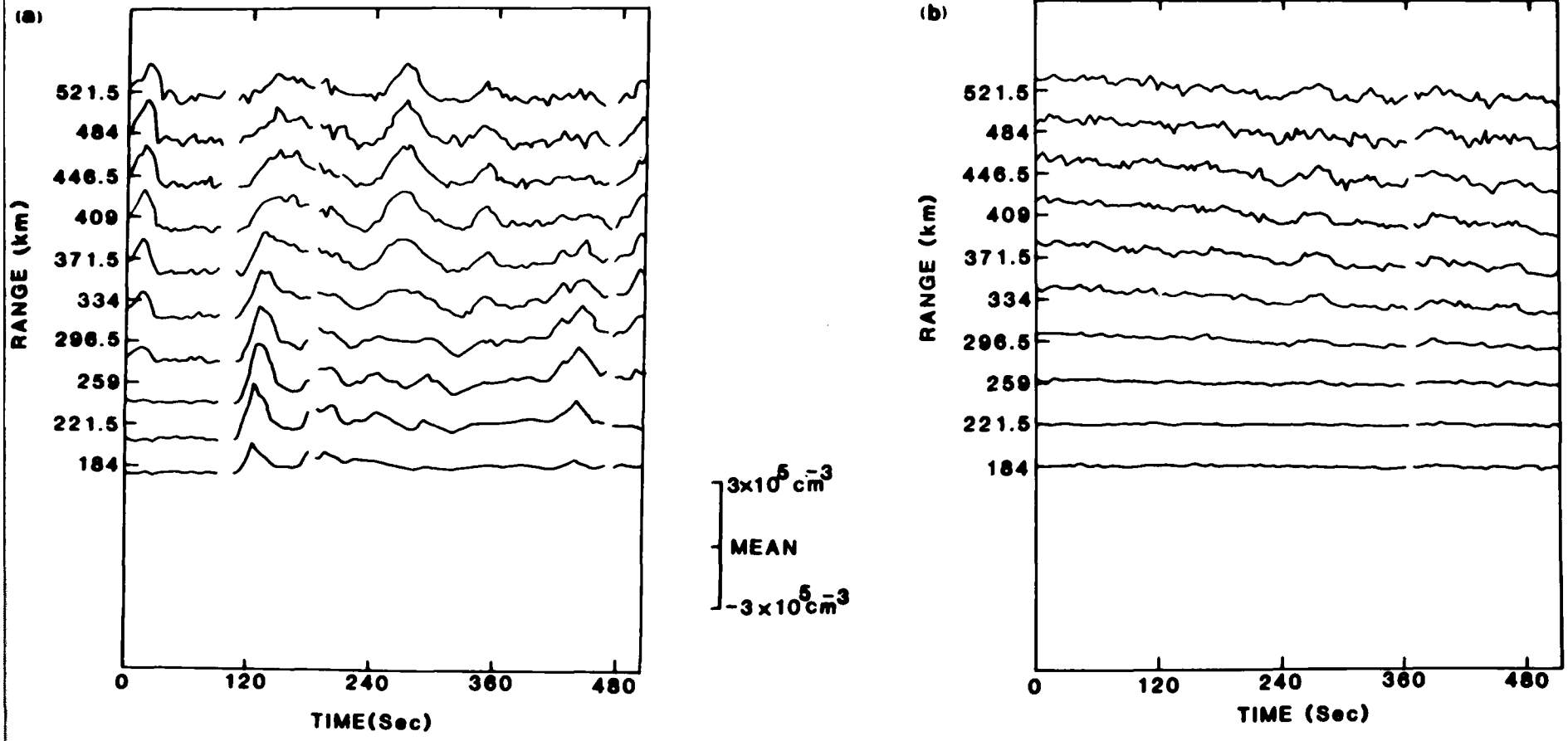
(a)
(b)
RANGE (km)
521.5
484
446.5
409
371.5
334
296.5
259
221.5
184
0
120
240
360
480
TIME(Sec)
TIME (Sec)
3x10^5 cm^-3
MEAN
-3x10^5 cm^-3

Fig. 3

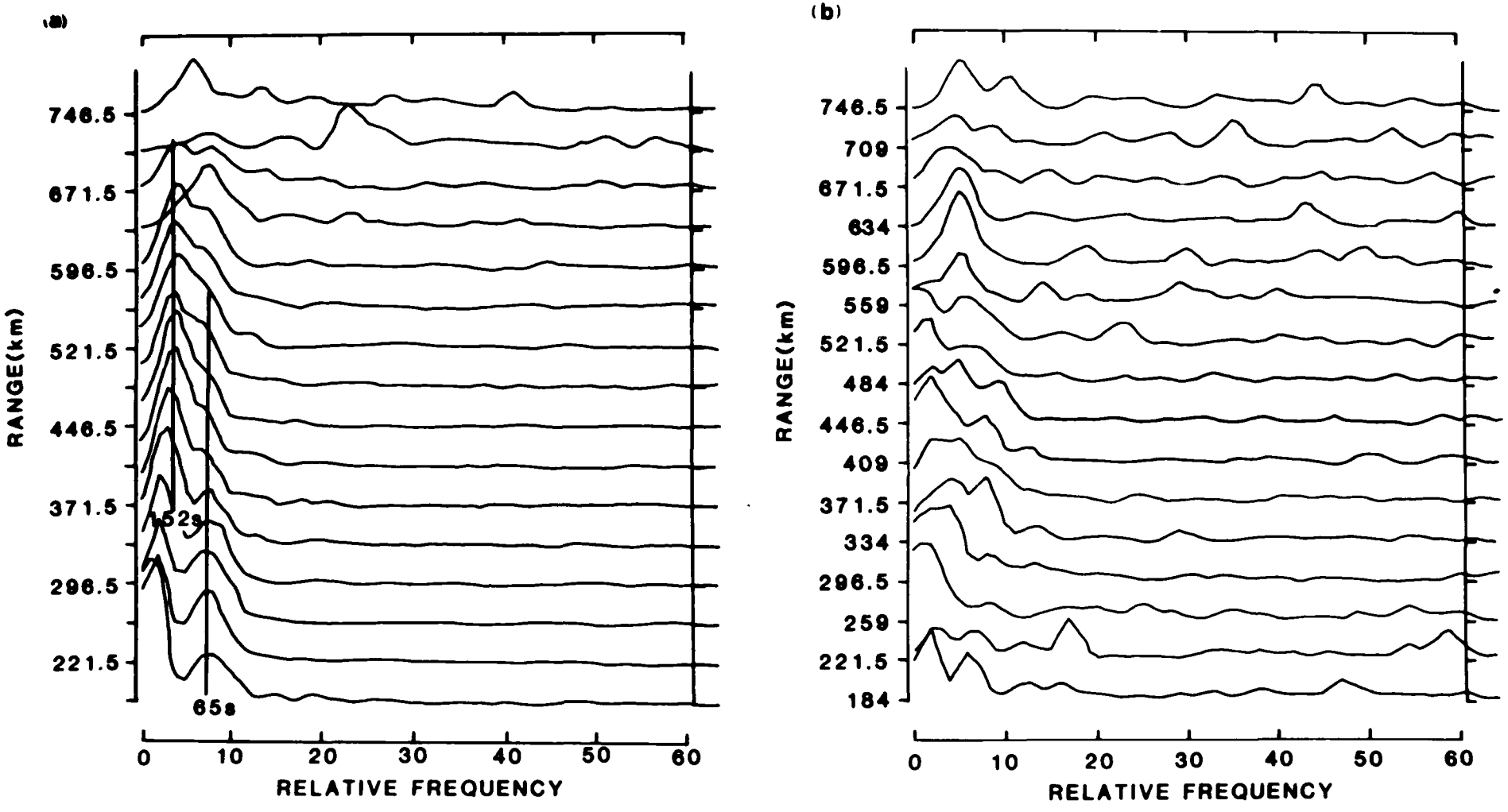
(a)
746.5
671.5
596.5
521.5
446.5
371.5
296.5
221.5
RANGE(km)
52s
65s
0
10
20
30
40
50
60
RELATIVE FREQUENCY
(b)
746.5
709
671.5
634
596.5
559
521.5
484
446.5
409
371.5
334
296.5
259
221.5
184
RANGE(km)
0
10
20
30
40
50
60
RELATIVE FREQUENCY

Fig. 4

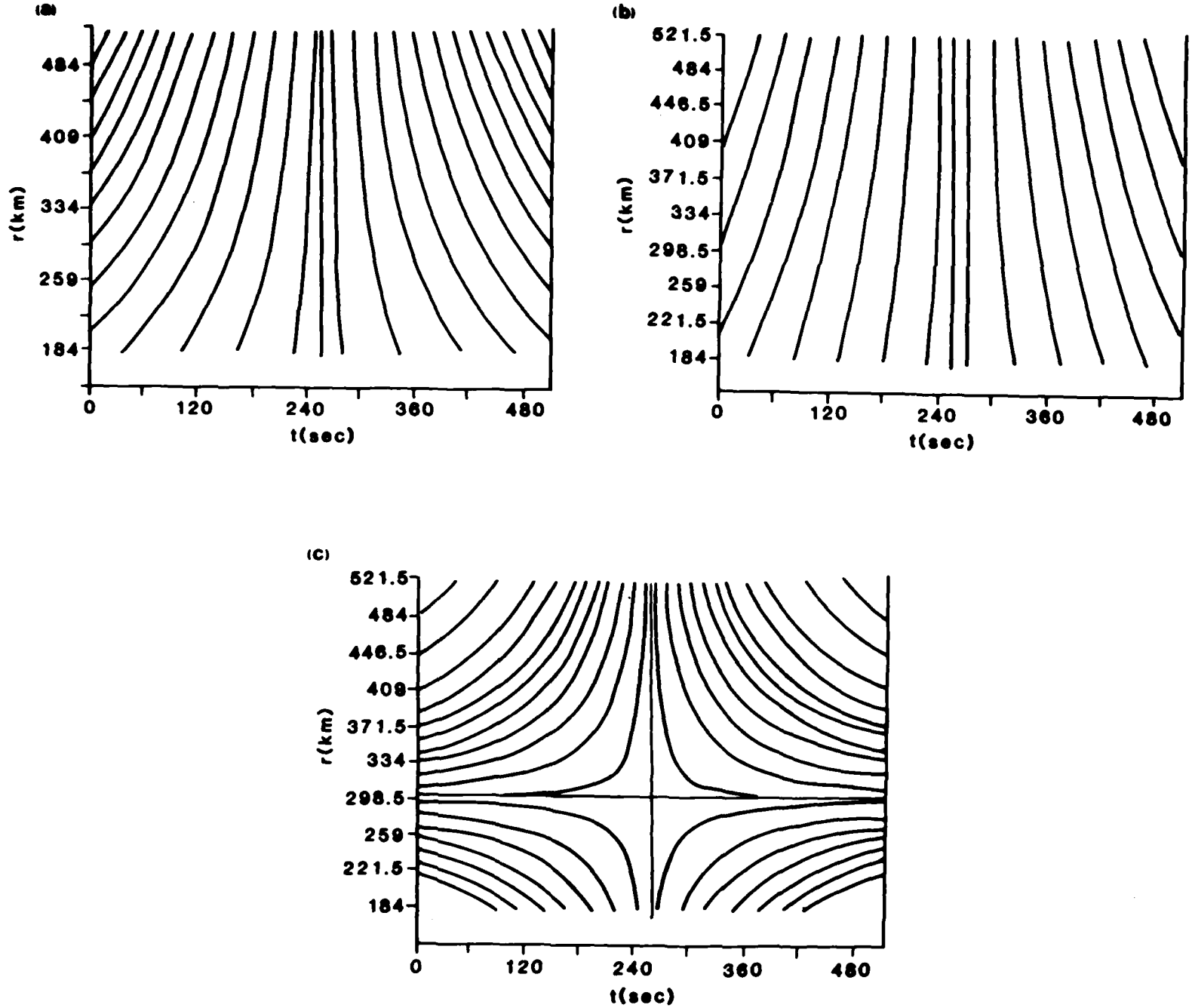
(a)
484
409
334
259
184
r(km)
0
120
240
360
480
t(sec)
(b)
521.5
484
446.5
409
371.5
334
298.5
259
221.5
184
r(km)
0
120
240
360
480
t(sec)
(c)
521.5
484
446.5
409
371.5
334
298.5
259
221.5
184
r(km)
0
120
240
360
480
t(sec)

Fig. 5

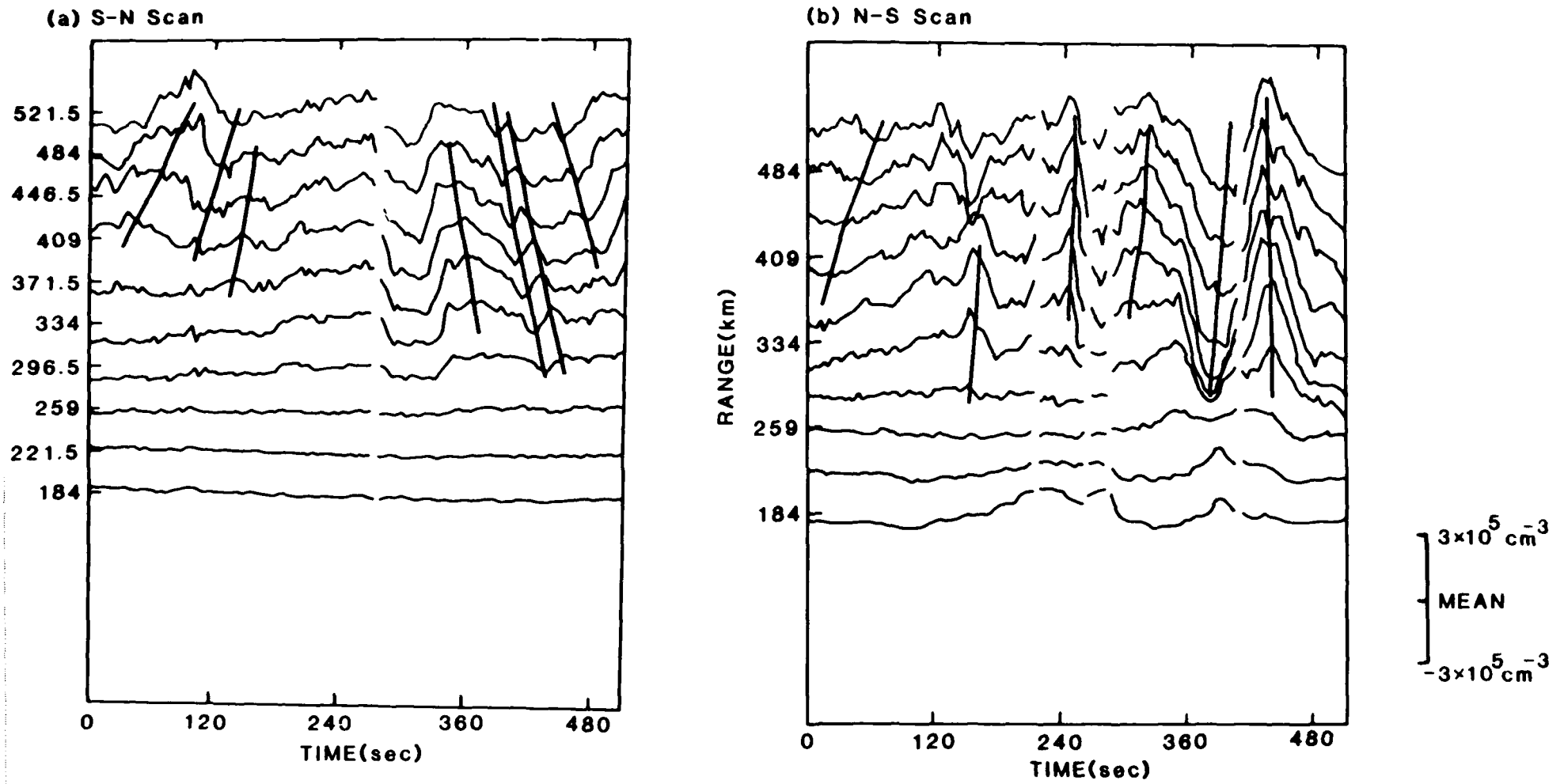
(a) S-N Scan
521.5
484
446.5
409
371.5
334
296.5
259
221.5
184
0
120
240
360
480
TIME(sec)
(b) N-S Scan
RANGE(km)
484
409
334
259
184
0
120
240
360
480
TIME(sec)
3×10^5 cm^-3
MEAN
-3×10^5 cm^-3

Fig. 6

Appendix 2: PROGRAMS

The following new programs have been written during the reporting period.

DENACF

This program plots 4-second resolution time-series of dNe/Ne (%) for each range. The program then determines the autocorrelation function for each of the time-series from lag zero up to lag 30. These are then plotted. The user has the option of leaving the data untreated, filtering it or detrending it. The filter used is a simple moving point average. The detrending involves the removal of the mean linear trend from the time series. The plots can be produced on one of several output devices, either hardcopy or VDU screen.

DENPSD

Plots time series similar to DENACF with the same treatment options. The program then determines the normalised power spectral density estimates for each range using a selected Tukey-Hanning window. Estimates are displayed between the Nyquist frequency and zero. The plots can be produced on one of several output devices.

DENSTAT

This program calculates various statistics of the 4-second resolution electron density data. For each range the program calculates the mean Ne (M), the standard deviation of Ne (SD), the variance of Ne (V) and the ratio SD/M.

The time series are then filtered using an arbitrary moving point average. The program calculates the filtered standard deviation (FSD), the filtered variance (FV) and finally the ratio FSD/M. These statistics are then printed to a file for hardcopy.

Table 1 summarises the main software now available for the analysis of data from SP 103.

Table 1 of Appendix 2

Data Processing Software for SP103

PROGRAM NAME	ROUTINES CALLED	DESCRIPTION	AUTHOR(S)
SYMBOUT		Prints text files from EISCAT raw data tapes	RAL EISCAT group
TAPEDAT	RNORD (ASSEM)	Reads raw data files from EISCAT tapes and stores to temporary disk.	RAL EISCAT group
ZLAGEX	RNORD	Extracts zero-lag acf's and system parameter information from the temporary disk files. Reduced data stored on permanent disk.	S.C. Kirkwood C.J. Burns
ZLAGCK	SMOG GRAPHICS	Cleans zero-lag acf's and averages background and calibration gates. Cleans transmitter power. Integrates over 3 frequences.	S.C. Kirkwood C.J. Burns
ZLAGPR		Reduces zero-lag acf's to pseudo-electron densities.	S.C. Kirkwood C.J. Burns
PROFPLOT	SMOG GRAPHICS	Produces profiles of electron density.	S.C. Kirkwood
DENACF	G13ABF (NAG) GINO GRAPHICS	Processes electron densities to give correlograms for each range with options to filter or detrend. Plots multiple time-series & correlograms. Outputs file of the correlogram data.	C.J. Burns

Table 1 (Contd.)

Data Processing Software for SP103

PROGRAM NAME	ROUTINES CALLED	DESCRIPTION	AUTHOR(S)
DENPSD	G13CAF (NAG) GINO GRAPHICS	Processes electron densities to give power spectral density estimates for each range. Options to filter or detrend data. Plots multiple time-series & periodograms. Outputs file of the periodogram data.	C.J. Burns
DENSTAT		Processes electron densities to give statistics for each range.	C.J. Burns
EISFREN		EISCAT front-end analysis program for determining data with 2 or more minutes post-integration.	RAL EISCAT group
GPLOT3	SMOG GRAPHICS	Plots electron densities and % variations as a function of time and range. Output can be on VDU or via FR80 film camera to film, paper or microfiche. (Note: FR80 no longer available at RAL).	S.C. Kirkwood C.M. Hall B.K. Madahar RAL systems group

END

FILMED

5-85

DTIC